Quark-hadron duality constraints on γZ box corrections to parity-violating elastic scattering

N. L. Hall[a], P. G. Blunden[a], W. Melnitchouk[b], A. W. Thomas[c], R. D. Young[c]

[a] *Department of Physics and Astronomy, University of Manitoba, Winnipeg, MB, Canada R3T 2N2*
[b] *Jefferson Lab, 12000 Jefferson Avenue, Newport News, Virginia 23606, USA*
[c] *ARC Centre of Excellence for Particle Physics at the Terascale and CSSM, Department of Physics, University of Adelaide, Adelaide SA 5005, Australia*

arXiv:1504.03973v2 [nucl-th] 25 Nov 2015

Abstract

We examine the interference γZ box corrections to parity-violating elastic electron–proton scattering in the light of the recent observation of quark-hadron duality in parity-violating deep-inelastic scattering from the deuteron, and the approximate isospin independence of duality in the electromagnetic nucleon structure functions down to $Q^2 \approx 1$ GeV^2. Assuming that a similar behavior also holds for the γZ proton structure functions, we find that duality constrains the γZ box correction to the proton's weak charge to be $\Re e\,\Box^V_{\gamma Z} = (5.4 \pm 0.4) \times 10^{-3}$ at the kinematics of the $Q_{\rm weak}$ experiment. Within the same model we also provide estimates of the γZ corrections for future parity-violating experiments, such as MOLLER at Jefferson Lab and MESA at Mainz.

Keywords: Parity violation, proton weak charge, quark-hadron duality

1. Introduction

Parity-violating precision measurements have for many years provided crucial low-energy tests of the Standard Model. Early efforts such as the E122 experiment at SLAC [1, 2] firmly established the SU(2)×U(1) model as the theory of the unified electroweak interactions. Modern-day experiments use parity violation to probe physics beyond the Standard Model. One of the most recent parity-violating measurements is the $Q_{\rm weak}$ experiment at Jefferson Lab [3], which aims to measure the proton's weak charge to 4% accuracy. With an initial analysis of a subset of the data already reported [4], the analysis of the full data set is expected in the near future.

For the precision requirements of the $Q_{\rm weak}$ experiment, the weak charge of the proton, defined at tree level as $Q_W^p = 1 - 4\sin^2\theta_W$, must also include radiative corrections. Including these corrections at the 1-loop level, the weak charge can be written as [5]

$$Q_W^p \;=\; (1 + \Delta\rho + \Delta_e)\left(1 - 4\sin^2\theta_W(0) + \Delta_e^{'}\right) + \Box_{WW} + \Box_{ZZ} + \Box_{\gamma Z}(0), \qquad (1)$$

where $\sin^2\theta_W(0)$ is the weak mixing angle at zero momentum transfer, and the electroweak vertex and neutral current correction terms $\Delta\rho$, Δ_e and Δ_e' have been calculated to the necessary levels of precision [5]. The weak box corrections $\Box_{WW}$ and $\Box_{ZZ}$ are dominated by short-distance effects and can also be computed perturbatively to the required accuracy.

On the other hand, the final term in Eq. (1), the γZ box contribution, depends on both short- and long-distance physics and therefore requires nonperturbative input. Considerable attention has been given to the analysis of this term, for both the vector electron–axial vector hadron coupling to the Z, $\Box^A_{\gamma Z}$ (which is relevant for atomic parity violation experiments) [6, 7, 8, 9], and the axial electron–vector hadron coupling, $\Box^V_{\gamma Z}$ (which because of its strong energy dependence makes important contributions to the $Q_{\rm weak}$ experiment) [10, 11, 12, 13, 14]. The most accurate technique to evaluate the latter is a dispersion relation. While constraints from parton distribution functions (PDFs) and recent parity-violating deep-inelastic scattering (PVDIS) data [15, 16] provide a systematic way of reducing the errors on this correction [14], some uncertainty remains about the model dependence of the low-Q^2 input.

The E08-011 electron–deuteron PVDIS experiment at Jefferson Lab not only allowed an accurate determination of the C_{2q} electron–quark effective weak couplings [16], but also presented the first direct evidence for quark-hadron duality in γZ interference structure functions, which was verified at the (10–15)% level for Q^2 down to ≈ 1 GeV^2 [15]. In general, quark-hadron duality refers to the similarity of low-energy hadronic cross sections, averaged over resonances, with asymptotic cross sections, calculated at the parton level and extrapolated to the resonance region. It is manifested in many different hadronic observables [17] and was first observed in deep-inelastic scattering (DIS) by Bloom and Gilman [18, 19]. Subsequent studies have quantified the validity of duality for various spin-averaged and spin-dependent electromagnetic structure functions, as well as in neutrino scattering and for different targets [20, 21, 22, 23, 24, 25, 26, 27], establishing the phenomenon as a general feature of the strong interaction.

Furthermore, recent analysis of moments of the free neutron electromagnetic structure function [28] has demonstrated that duality in the lowest three neutron moments is violated at a similar level ($\lesssim 10\%$) as in the proton for $Q^2 \geqslant 1$ GeV^2 [20, 21, 26]. This suggests that the isospin dependence of duality and its violation is relatively weak. It is reasonable therefore to expect that duality may also hold to a similar degree for the γZ structure functions, which are related to the electromagnetic structure functions by isospin rotations.

In this paper we discuss the extent to which quark-hadron duality in γZ structure functions can provide additional constraints on the $\Box^V_{\gamma Z}$ corrections, and in particular the contributions from low hadronic final state masses W and $Q^2 \sim 1$ GeV^2. In Sec. 2 we illustrate the realization of duality in the moments of the proton and neutron electromagnetic structure functions using empirical parametrizations of data in the resonance and DIS regions down to $Q^2 = 1$ GeV^2. Motivated by the approximate isospin independence of duality in electromagnetic scattering from the nucleon, in Sec. 3 we explore the consequences of duality in the γZ structure functions for the energy dependence of the $\Box^V_{\gamma Z}$ correction, and especially the limits on its overall uncertainty. Finally, in Sec. 4 we summarize our findings and discuss their implications for the analysis of the $Q_{\rm weak}$ experiment as well as future parity-violating experiments such as MOLLER at Jefferson Lab [29] and MESA at Mainz [30].

2. Duality in electromagnetic structure functions

Historically, the observation of duality in inclusive electron scattering [18, 19] predates the development of QCD and was initially formulated in the language of finite-energy sum rules. Within QCD, duality was reinterpreted within the operator product expansion through moments of structure functions [31], with duality violations associated with matrix elements of higher twist (HT) operators describing multi-parton physics. The extent to which inclusive lepton–nucleon cross sections can be described by incoherent scattering from individual partons through leading twist (LT) PDFs can be quantified by studying the Q^2 dependence of the structure function moments. At low Q^2, corrections to the LT results arise not only from multi-parton processes, but also from kinematical target mass corrections (TMCs), which, although $1/Q^2$ suppressed, arise from LT operators. To isolate the genuine duality-violating HT effects, one can consider Nachtmann moments of structure functions [32], which are constructed to explicitly remove the effects of higher spin operators and the resulting TMCs.

Specifically, the Nachtmann moments of the F_1 and F_2 structure functions are defined as [33, 34]

$$\mu_1^{(n)}(Q^2) = \int_0^1 dx\, \frac{\xi^{n+1}}{x^3} \left[x F_1(x,Q^2) + \frac{1}{2}\rho^2 \eta_n F_2(x,Q^2) \right], \tag{2}$$

$$\mu_2^{(n)}(Q^2) = \int_0^1 dx\, \frac{\xi^{n+1}}{x^3}\, \rho^2 (1+3\eta_n) F_2(x,Q^2), \tag{3}$$

where

$$\xi = \frac{2x}{1+\rho} \tag{4}$$

is the Nachtmann scaling variable [33, 35], with $x = Q^2/(W^2 - M^2 + Q^2)$ the Bjorken scaling variable, $\rho^2 = 1 + 4M^2x^2/Q^2$, and M the nucleon mass. The variable η_n is given by

$$\eta_n = \frac{\rho - 1}{\rho^2} \left[\frac{n + 1 - (\rho+1)(n+2)}{(n+2)(n+3)} \right], \tag{5}$$

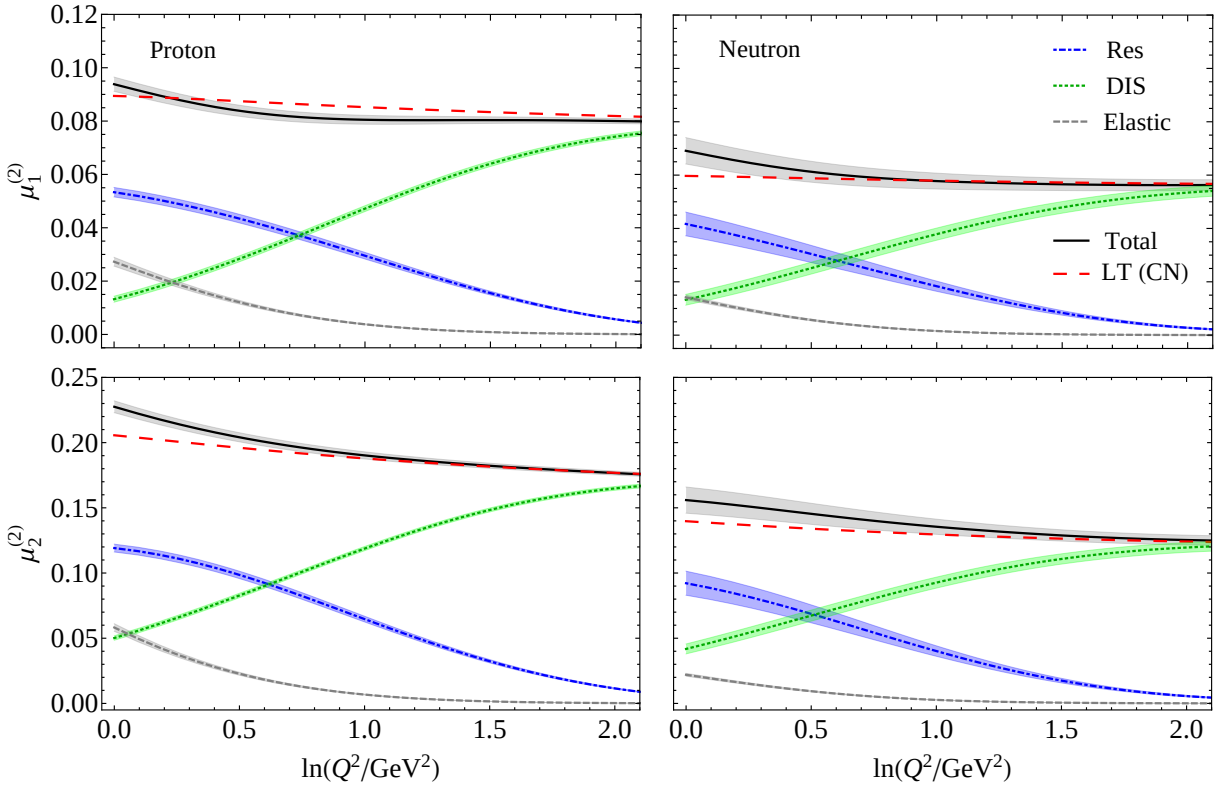


Figure 1: The proton (left panels) and neutron (right panels) electromagnetic $F_1^{\gamma\gamma}$ (top) and $F_2^{\gamma\gamma}$ (bottom) structure function moments. The total Nachtmann moments (black solid lines) include contributions from the resonance ($W^2 \leqslant 6$ GeV^2, blue dot-dashed lines) and DIS ($W^2 > 6$ GeV^2, green dotted lines) regions, as well as the elastic contributions (gray dashed lines), and are compared with the Cornwall-Norton moments of the LT structure functions (red long-dashed lines).

and vanishes in the $Q^2 \to \infty$ limit. In that limit the moments $\mu_i^{(n)}$ approach the standard Cornwall-Norton moments [36],

$$\mu_i^{(n)}(Q^2) \quad \longrightarrow \quad M_i^{(n)}(Q^2) \;=\; \int_0^1 dx\, x^{n-i}\, F_i(x, Q^2), \qquad i = 1, 2. \tag{6}$$

At finite Q^2, while the $\mu_2^{(n)}$ moments depend only on the F_2 structure function, the $\mu_1^{(n)}$ moments have contributions from both the F_1 and F_2 structure functions. Because the latter contribution is proportional to η_n, it vanishes at large Q^2, so that the $\mu_1^{(n)}$ moments are generally dominated by the F_1 structure function at large Q^2.

Duality in unpolarized electron–nucleon scattering has been studied most extensively for the electromagnetic F_2 structure function [20, 21, 26], and to a lesser extent for the F_1 (or longitudinal F_L) structure function [17, 37]. The latter is generally more difficult to access experimentally, as it requires precise longitudinal–transverse separated cross section measurements, or equivalently the σ_L/σ_T cross section ratio. In Fig. 1 the workings of duality in the $n = 2$ Nachtmann moments of the proton and neutron $F_1^{\gamma\gamma}$ and $F_2^{\gamma\gamma}$ structure functions are illustrated over the range $1 \leqslant Q^2 \leqslant 8$ GeV^2. For the low-W^2 contributions, $W^2 \leqslant 6$ GeV^2, the resonance-based fit to the electromagnetic structure function data from Christy and Bosted [38] is used. For the DIS region at higher W^2 values, $W^2 > 6$ GeV^2, this is supplemented by the ABM global QCD fit [39] to high-energy data, which includes LT, TMC and HT contributions. Since LT evolution is logarithmic in Q^2, at large Q^2 the moments are predicted to become flat in $\ln Q^2$. While the individual resonance and DIS region contributions, as well as the elastic ($W = M$) component, are strongly Q^2 dependent in the region of low Q^2 shown in Fig. 1, remarkably their sum exhibits only very mild Q^2 dependence down to

$Q^2 \approx 1$ GeV^2. This is the classic manifestation of duality observed by Bloom and Gilman [18, 19], in which the total empirical moments resemble the LT contributions down to surprisingly low momentum scales. Note that since the Nachtmann moments are constructed to remove higher spin operators that are responsible for TMCs, in the absence of HTs one would expect the Nachtmann moments of the total structure functions to equal the Cornwall-Norton moments of the LT functions, $\mu_i^{(n)}(\mathrm{LT}+\mathrm{TMC}) = M_i^{(n)}(\mathrm{LT})$ [40].

This expectation is clearly borne out in Fig. 1, where the total $\mu_1^{(2)}$ and $\mu_2^{(2)}$ moments are very similar to the moments computed from the LT PDFs. For the proton structure functions, the average violation of duality in the range $1 \leqslant Q^2 \leqslant 2.5$ GeV^2 is 3% and 4% for the $F_1^{\gamma\gamma}$ and $F_2^{\gamma\gamma}$ structure functions, respectively, with the maximum violation being $\approx 5\%$ and $\approx 10\%$ at the lower end of the Q^2 range. For the neutron the maximum violation is slightly larger, with the LT $F_1^{\gamma\gamma}$ and $F_2^{\gamma\gamma}$ moments being $\approx 14\%$ and $\approx 10\%$ smaller than the full results, although the average over this Q^2 range is 5% and 8%, respectively. This is consistent with several previous phenomenological analyses [41, 42, 43] of high-energy scattering data which have found no indication of strong isospin dependence of HT corrections. Following Ref. [38], we assign a 5% error on the proton $F_1^{\gamma\gamma}$ and $F_2^{\gamma\gamma}$ structure functions, and a larger, 10% error on the neutron structure function [44], reflecting the additional nuclear model dependence in extracting the latter from deuterium data [45]. For the elastic contribution a 5% uncertainty is assumed for the total elastic structure functions from Ref. [46]. For higher moments ($n > 2$), which are progressively more sensitive to the high-x (or low-W) region, the degree to which duality is satisfied diminishes at lower Q^2 values [47].

3. Duality in γZ structure functions and implications for Q_W^p

In contrast to the electromagnetic structure functions which have been studied extensively for many years, experimental information on the interference γZ structure functions is for the most part nonexistent. Some measurements of $F_2^{\gamma Z}$ and $xF_3^{\gamma Z}$ have been made at very high Q^2 at HERA [48], where the γZ contribution becomes comparable to the purely electromagnetic component of the neutral current. However, no direct measurements of $F_1^{\gamma Z}$ and $F_2^{\gamma Z}$ for the proton exist in the $Q^2 \sim$ few GeV^2 range relevant for the evaluation of the γZ box correction to Q_W^p [14].

In principle, the computation of the imaginary part of the $\Box_{\gamma Z}^V$ correction to the proton's weak charge at a given incident energy E requires knowledge of the γZ structure functions over all kinematics,

$$\Im m\,\Box_{\gamma Z}^V(E) \;=\; \frac{1}{(s-M^2)^2}\int_{W_\pi^2}^{s} dW^2 \int_0^{Q^2_{\rm max}} dQ^2\, \frac{\alpha(Q^2)}{1+Q^2/M_Z^2}\left[F_1^{\gamma Z} + \frac{s\left(Q^2_{\rm max}-Q^2\right)}{Q^2\left(W^2-M^2+Q^2\right)}F_2^{\gamma Z}\right]. \qquad (7)$$

where α is the running electromagnetic coupling evaluated at the scale Q^2, and M_Z is the Z boson mass. The W^2 range covered in the integral lies between the inelastic threshold, $W_\pi^2 = (M+m_\pi)^2$ and the total electron–proton center of mass energy squared, $s = M^2 + 2ME$, while the Q^2 integration range is from 0 up to $Q^2_{\rm max} = 2ME(1-W^2/s)$. (The small mass of the electron is neglected throughout.) The real part of the γZ box correction which enters in Eq. (1) can then be determined from the imaginary part through an unsubtracted dispersion relation [10, 11, 12, 13, 14],

$$\Re e\,\Box_{\gamma Z}^V(E) \;=\; \frac{2E}{\pi}\mathcal{P}\int_0^\infty dE' \frac{1}{E'^2-E^2}\,\Im m\,\Box_{\gamma Z}^V(E'), \qquad (8)$$

where $\mathcal{P}$ is the Cauchy principal value integral. While the dispersion relation (8) is valid only for forward scattering, because the $Q_{\rm weak}$ experiment is performed at a small scattering angle $\approx 6^\circ$, in practice it provides a very good approximation.

Note that at high Q^2 and large E, the total correction $\Re e\,\Box_{\gamma Z}^V$ can also be expressed in terms of the moments of the $F_1^{\gamma Z}$ and $F_2^{\gamma Z}$ structure functions by switching the order of the integrations in Eqs. (7) and (8) and expanding the integrand in powers of x^2/Q^2 [8]. The higher order terms in $1/Q^2$ are then given in terms of higher moments of the structure functions. The expansion in Ref. [8] was performed in terms of the Cornwall-Norton moments, but the expansion could also be generalized to the Nachtmann moments in Eqs. (2) and (3). However, because this approximation neglects contributions from the low-W region, it is appropriate only for DIS kinematics and is not directly applicable for the present application, where the integrals are dominated by contributions at low Q^2 and W^2. In particular, as we discuss below, at energy

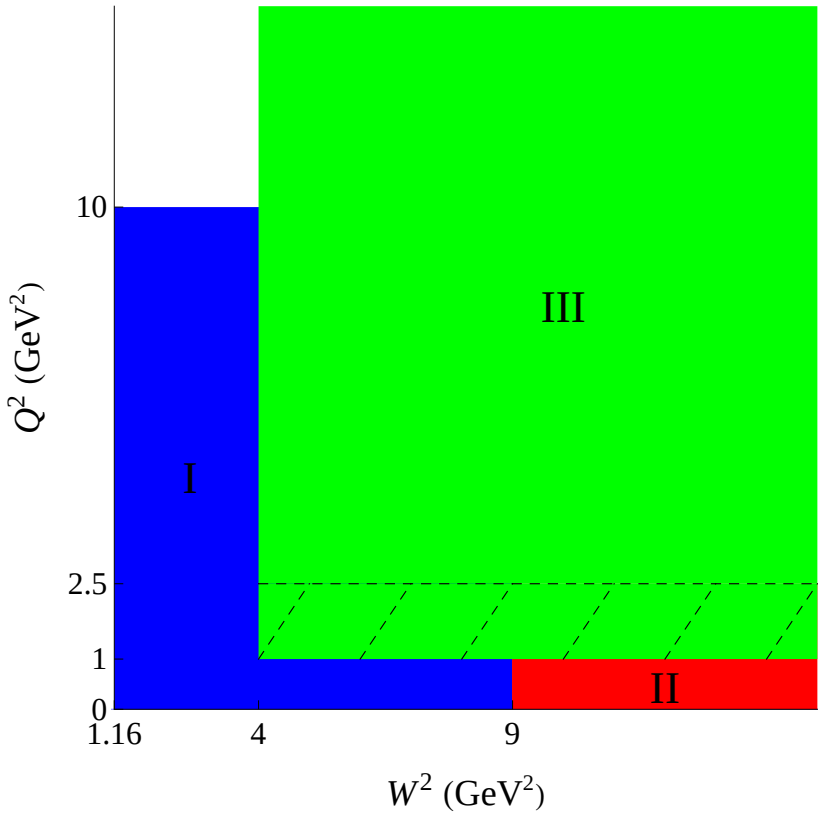


Figure 2: Kinematic regions contributing to the $\Box^V_{\gamma Z}$ integrals in the AJM model. Region I (blue) includes the nucleon resonance region at low W^2 and Q^2; Region II (red) encompasses the low-Q^2, high-W^2 region described by Regge theory; and Region III (green) is the deep-inelastic region characterized by LT PDFs. The shaded band between $Q^2 = 1$ and 2.5 GeV^2 represents the extension of Region III from its previous boundary in Ref. [14] ($Q^2 = 2.5$ GeV^2) to its current reach ($Q^2 = 1$ GeV^2).

$E \sim 1$ GeV, approximately 2/3 of the integral comes from the traditional resonance region $W < 2$ GeV and $Q^2 < 1$ GeV^2. In contrast, the contribution from the DIS region for $W > 2$ GeV and $Q^2 > 1$ GeV^2 is $\approx 13\%$ at this energy.

In Refs. [14, 50] the $F_1^{\gamma Z}$ and $F_2^{\gamma Z}$ structure functions were computed from the phenomenological Adelaide-Jefferson Lab-Manitoba (AJM) parametrization. This is based on the electromagnetic structure functions described in Sec. 2, but appropriately rotated to the γZ case according to the specific W^2 and Q^2 region considered, with the rotation parameters constrained by phenomenological PDFs [14] and recent PVDIS data [15, 16]. In the AJM model the integrals over W^2 and Q^2 in Eq. (7) are split into three distinct regions, characterized by different physical mechanisms underlying the scattering process. In each region the most accurate parametrizations or models of $F_1^{\gamma Z}$ and $F_2^{\gamma Z}$ available for the appropriate kinematics are used.

In the present analysis, we define the W^2 and Q^2 regions as illustrated in Fig. 2. "Region I" (low Q^2, low W^2) encompasses $0 \leqslant Q^2 \leqslant 10$ GeV^2 for $W_\pi^2 \leqslant W^2 \leqslant 4$ GeV^2, and $0 \leqslant Q^2 \leqslant 1$ GeV^2 for $4 < W^2 \leqslant 9$ GeV^2, using the $\gamma\gamma \to \gamma Z$ rotated Christy-Bosted parametrization [38] of the resonance + background structure functions. For "Region II" (low Q^2, high W^2), the vector meson dominance + Regge model of Alwall and Ingelman [49] is used over the range $0 \leqslant Q^2 \leqslant 1$ GeV^2 and $W^2 > 9$ GeV^2. Finally, for "Region III" (high Q^2, high W^2) the perturbative QCD-based global fit from Alekhin *et al.* (ABM) [39] is used for $Q^2 > 1$ GeV^2 and $W^2 > 4$ GeV^2, which includes LT as well as subleading $1/Q^2$ TMC and HT contributions. For $x = 1$, the elastic contributions to the structure functions are computed using the form factor parametrizations from Ref. [46].

While the uncertainties on the γZ structure functions in Region III are small — typically a few %, reflecting the errors on the PDFs from which they are constructed through the simple replacement of quark charges $e_q \to g_V^q$ — the uncertainties in $F_1^{\gamma Z}$ and $F_2^{\gamma Z}$ are expected to be larger at lower W^2 and Q^2. In the

previous analyses of the γZ correction [14, 50], the PDF-based description was limited to $Q^2 > 2.5$ GeV^2 (and $W^2 > 4$ GeV^2). Motivated by the observation of duality in the proton and neutron $F_1^{\gamma\gamma}$ and $F_2^{\gamma\gamma}$ structure functions, and in PVDIS from the deuteron, as discussed in Sec. 2, we further assume the approximate validity of duality in the γZ proton structure functions and extend the QCD description of Region III down to $Q^2 = 1$ GeV^2. Lowering the boundary of the DIS region, which is well constrained by leading twist PDFs, to smaller Q^2 decreases the contribution from Regions I and II, and hence reduces the model uncertainty on the $\gamma\gamma \to \gamma Z$ rotation of the structure functions in this region.

Within the AJM γZ structure function parametrization, the most uncertain elements are the $\kappa_C^{T,L}$ continuum parameters used to relate the high-mass, non-resonant continuum part of the γZ transverse and longitudinal cross sections to the $\gamma\gamma$ cross sections in the generalized vector meson dominance model [49, 51]. The $\kappa_C^{T,L}$ parameters are fitted by matching the γZ to $\gamma\gamma$ cross section ratios with the LT structure function ratios at $Q^2 = 1$ GeV^2,

$$\frac{\sigma_T^{\gamma Z}(\kappa_C^T)}{\sigma_T^{\gamma\gamma}} \;=\; \left.\frac{F_1^{\gamma Z}}{F_1^{\gamma\gamma}}\right|_{\rm LT}, \qquad\qquad \frac{\sigma_L^{\gamma Z}(\kappa_C^L)}{\sigma_L^{\gamma\gamma}} \;=\; \left.\frac{F_L^{\gamma Z}}{F_L^{\gamma\gamma}}\right|_{\rm LT}, \tag{9}$$

where the longitudinal structure function F_L is related to the F_1 and F_2 structure functions by $F_L = \rho^2 F_2 - 2xF_1$ [14]. (Note that, consistent with the duality hypothesis, we use the LT structure functions in Region III rather than the total structure functions that may include the small subleading contributions [39].) The resulting fit values,

$$\kappa_C^T \;=\; 0.36 \pm 0.15, \qquad\qquad \kappa_C^L \;=\; 1.5 \pm 3.1, \tag{10}$$

are obtained by averaging over the $\kappa_C^{T,L}$ parameter determined from 10 fits with the ratios in Eq. (9) matched at between $W^2 = 4$ GeV^2 and 13 GeV^2. These values are then used to compute the γZ structure functions in the dispersion integral for $1 \leqslant Q^2 \leqslant 10$ GeV^2 and $W_\pi^2 \leqslant W^2 \leqslant 4$ GeV^2. To allow for stronger violations of duality at lower Q^2, the uncertainties on $\kappa_C^{T,L}$ are inflated to 100% for the region $0 \leqslant Q^2 < 1$ GeV^2 for all W^2. In the numerical calculations the uncertainties on the proton γZ structure function parametrizations are taken to be the same as those used in the $\Box_{\gamma Z}^V$ calculation in Ref. [14], and a 5% uncertainty is assumed for the nucleon elastic contributions.

Using the γZ structure functions obtained from the newly fitted $\kappa_C^{T,L}$ values, the $\Re e\,\Box_{\gamma Z}^V$ correction is displayed in Fig. 3 as a function of beam energy, with a breakdown of the individual contributions from different regions given in Table 1. At the incident beam energy $E = 1.165$ GeV of the $Q_{\rm weak}$ experiment, the total correction is found to be

$$\Re e\,\Box_{\gamma Z}^V \;=\; (5.4 \pm 0.4) \times 10^{-3}. \tag{11}$$

This is in good agreement with the value $\Re e\,\Box_{\gamma Z}^V = (5.57 \pm 0.36) \times 10^{-3}$ found in the previous analysis [14]. In particular, even though the values of the continuum rotation parameters in the earlier fit were somewhat different ($\kappa_C^T = 0.65 \pm 0.14$ and $\kappa_C^L = -1.3 \pm 1.7$ with matching to the total DIS structure functions at $Q^2 = 2.5$ GeV^2), the central value of $\Re e\,\Box_{\gamma Z}^V$ remains relatively unaffected.

Table 1: Contributions to $\Re e\,\Box_{\gamma Z}^V$ from Regions I, II and III, and the total, at the kinematics of the $Q_{\rm weak}$, MOLLER, and MESA experiments.

	$\Re e\,\Box_{\gamma Z}^V$ ($\times 10^{-3}$)		
Region	$Q_{\rm weak}$ ($E = 1.165$ GeV)	MOLLER ($E = 11$ GeV)	MESA ($E = 0.18$ GeV)
I	4.3 ± 0.4	2.5 ± 0.3	1.0 ± 0.1
II	0.4 ± 0.05	3.2 ± 0.5	0.06 ± 0.01
III	0.7 ± 0.04	5.5 ± 0.3	0.1 ± 0.01
Total	5.4 ± 0.4	11.2 ± 0.7	1.2 ± 0.1

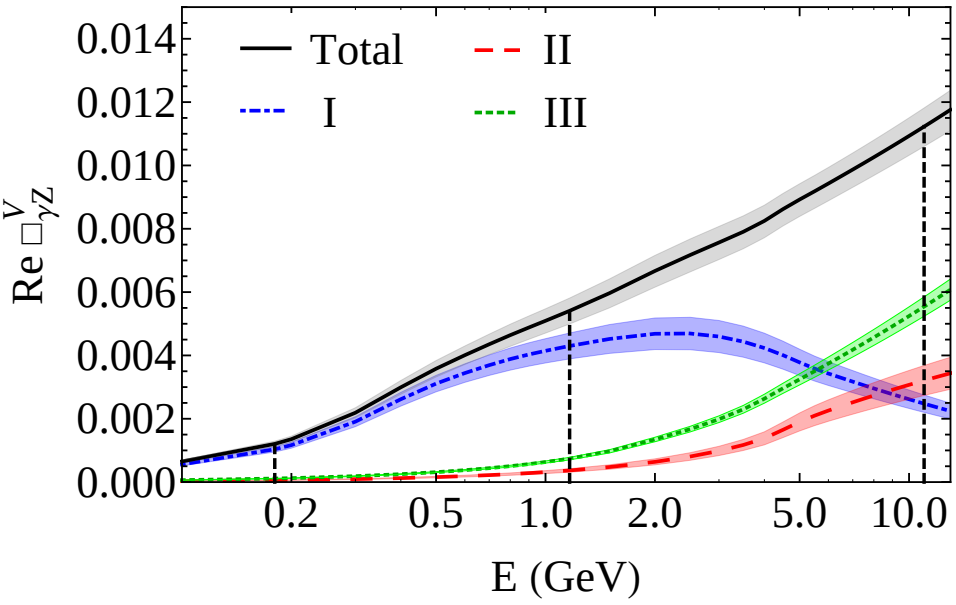


Figure 3: Energy dependence of the γZ box correction, $\Re e\,\Box^V_{\gamma Z}$, to Q^p_W. The contributions from various regions in W^2 and Q^2 (Regions I, II and III) are shown separately, as is the total (solid curve). The dashed vertical lines indicate the beam energies of the various parity-violating experiments ($E = 0.18$ GeV for MESA [30], $E = 1.165$ GeV for $Q_{\rm weak}$ [4], and $E = 11$ GeV for MOLLER [29].

The largest contribution to $\Re e\,\Box^V_{\gamma Z}$ at the $Q_{\rm weak}$ energy is still from Region I, which makes up $\approx 80\%$ of the total, with its error dominating the total uncertainty. Of this, $\approx 2/3$ is from the traditional resonance region $W^2 < 4$ GeV^2 (of which 61% is from $Q^2 < 1$ GeV^2 and 6% from $Q^2 > 1$ GeV^2), and $\approx 13\%$ is from $Q^2 < 1$ GeV^2 and $4 < W^2 < 9$ GeV^2. The contributions from Regions II and III are $\approx 7\%$ and $\approx 13\%$, respectively, of the total at the $Q_{\rm weak}$ energy, but become more important with increasing energy. Interestingly, the modified Q^2 boundary for Region III results in a somewhat smaller contribution from Region II (0.4×10^{-3} compared with 0.6×10^{-3}), while the Region III contribution has doubled (0.7×10^{-3} compared with 0.35×10^{-3}) relative to that in Ref. [14]. In effect, moving the Q^2 boundary from 2.5 GeV^2 to 1 GeV^2 shifts $\approx 6\%$ of the total correction $\Re e\,\Box^V_{\gamma Z}$ from Regions I and II to Region III.

Furthermore, since the γZ structure functions at $Q^2 < 1$ GeV^2 depend on $\kappa_C^{T,L}$, because the κ values are refitted at $Q^2 = 1$ GeV^2, duality also indirectly affects the low-Q^2 contribution. Therefore, although duality is formally used only down to $Q^2 = 1$ GeV^2, the constraint influences the γZ calculation below 1 GeV^2 as well, as the matching now is to a more reliable γZ cross section at that point.

While we have assumed the validity of duality for the $F_1^{\gamma Z}$ and $F_2^{\gamma Z}$ structure functions down to $Q^2 = 1$ GeV^2, the possible violations of duality have a minor effect on the analysis. Even if one takes the maximum violation of duality ($\approx 14\%$) in the $\gamma\gamma$ structure functions seen in Fig. 1 at the lowest Q^2 over the entire $1 \leqslant Q^2 \leqslant 2.5$ GeV^2 range, the error introduced into the total $\Re e\,\Box^V_{\gamma Z}$ from duality violation is $< 0.1\%$.

Overall, compared with Ref. [14] the total relative uncertainty increases marginally, from 6.5% to 7.4%, despite the rather more conservative estimates of the structure function uncertainty for $Q^2 \lesssim 1$ GeV^2 through the inflated errors on $\kappa_C^{T,L}$. Note that the same 100% uncertainties are used in the transformation of the vector meson dominance model [49, 51] in Region II. For Region III, the LT $F_1^{\gamma Z}$ and $F_2^{\gamma Z}$ structure functions are assigned a 5% uncertainty for $Q^2 \geqslant 2.5$ GeV^2, which is increased linearly to 10% at $Q^2 = 1.0$ GeV^2.

Since the electromagnetic structure functions are reasonably well approximated by the LT results even below the traditional resonance-DIS boundary of $W^2 = 4$ GeV^2, we also examine the effect of lowering the W^2 cut into the peripheral resonance region down to $W^2 = 3$ GeV^2. In this case the contribution from Region III increases to 0.9×10^{-3}, while that from Region I correspondingly decreases to 4.2×10^{-3}, hence

leaving the total essentially unchanged.

At the higher $E = 11$ GeV energy of the planned MOLLER experiment at Jefferson Lab [29], the DIS region contributes about half of the total, $\Re e\,\Box^V_{\gamma Z} = (11.2 \pm 0.7) \times 10^{-3}$, with Regions I and II making up the other 50%. This again agrees well with the earlier determination $\Re e\,\Box^V_{\gamma Z} = (11.5 \pm 0.8) \times 10^{-3}$ from Ref. [50]. On the other hand, for the possible future MESA experiment in Mainz [30] at a lower energy, $E = 0.18$ GeV, the bulk of the contribution still comes from Region I, but is reduced by a factor of ~ 4 compared with the correction at the $Q_{\rm weak}$ energy.

4. Conclusion

Quark-hadron duality is one of the most remarkable phenomena ever observed in hadronic physics. While some aspects of global duality can be formulated in the language of QCD, such as the relation between the scale independence of structure function moments and the size of higher twists, the detailed workings of local duality, for specific regions of W^2 or x, are not well understood from first principles. Nevertheless, there are many marvellous practical applications to which duality can be put. For example, the high-energy behavior of hadronic cross sections can be used to predict averages of resonance properties; and, conversely, low-W^2 data, suitably averaged, can be utilized to constrain LT parton distributions in difficult to access kinematic regions.

The latter category appears the most promising approach at present, with several global PDF analyses [39, 45, 43] extending their coverage down to lower Q^2 ($Q^2 \gtrsim 1$ GeV^2) and W^2 ($W^2 \gtrsim 3$ GeV^2) values than in traditional LT analyses. This not only increases considerably the available data base for PDF fitting, it is also one of the few ways currently available to study PDFs at high $x \sim 1$.

The main implication of duality for the current analysis is the extension of the LT description of γZ structure functions to lower Q^2, $Q^2 = 1$ GeV^2, than in previous work [14]. This serves to reduce the size of the contribution from Region I, which has the largest uncertainty associated with the behavior of the γZ structure functions at low Q^2 and W^2. To account for the possible model dependence of the $\gamma\gamma \to \gamma Z$ structure function rotation and the violation of duality at low Q^2, we have assigned rather conservative errors on $F_1^{\gamma Z}$ and $F_2^{\gamma Z}$ in this region. This is reflected in the increased uncertainty on this contribution compared with our previous analysis [14], which is somewhat offset by the larger contribution from Region III that is well constrained by PDFs.

The final result of $\Re e\,\Box^V_{\gamma Z} = (5.4 \pm 0.4) \times 10^{-3}$ is consistent with Ref. [14], but with a slightly larger relative uncertainty, which comes almost entirely from Region I. It also agrees with the central value from Ref. [13], although the error there is ≈ 5 times larger, which in view of our current analysis appears to be somewhat overestimated. Our findings suggest that with the constraints from existing PVDIS data and PDFs, and now with the further support from quark-hadron duality, the overall uncertainty in the estimate of the γZ box correction is well within the range needed for an unambiguous extraction of the weak charge from the $Q_{\rm weak}$ experiment.

Further reduction of the uncertainty on the γZ correction will come from new measurements of PVDIS asymmetries on the proton, particularly at the low Q^2 and W^2 values that are most relevant at the $Q_{\rm weak}$ energy. These will also be useful in constraining the γZ contribution at the much lower energy $E = 0.18$ GeV of the MESA experiment [30], where we find the correction to be ≈ 4 times smaller but even more dominated by Region I. In contrast, for the MOLLER experiment at the higher $E = 11$ GeV energy the dispersion integral is dominated by the DIS region, which although contributing to a larger overall $\Box^V_{\gamma Z}$ correction, is better determined in terms of PDFs. These new experiments hold the promise of allowing the most precise low-energy determination of the weak mixing angle to date, and providing a unique window on possible new physics beyond the Standard Model.

Acknowledgements

This work was supported by NSERC (Canada), the DOE Contract No. DE-AC05-06OR23177, under which Jefferson Science Associates, LLC operates Jefferson Lab, and the Australian Research Council through an Australian Laureate Fellowship (A.W.T.), a Future Fellowship (R.D.Y.) and through the ARC Centre of Excellence for Particle Physics at the Terascale.

References

[1] C. Y. Prescott *et al.*, Phys. Lett. B **77** (1978) 347.

[2] C. Y. Prescott *et al.*, Phys. Lett. B **84** (1979) 524.

[3] D. S. Armstrong *et al.*, arXiv:1202.1255.

[4] D. Androic *et al.*, Phys. Rev. Lett. **111** (2013) 141803.

[5] J. Erler, A. Kurylov and M. J. Ramsey-Musolf, Phys. Rev. D **68** (2003) 016006.

[6] W. J. Marciano and A. Sirlin, Phys. Rev. D **27** (1983) 552.

[7] W. J. Marciano and A. Sirlin, Phys. Rev. D **29** (1984) 75.

[8] P. G. Blunden, W. Melnitchouk and A. W. Thomas, Phys. Rev. Lett. **107** (2011) 081801.

[9] P. G. Blunden, W. Melnitchouk and A. W. Thomas, Phys. Rev. Lett. **109** (2012) 262301.

[10] M. Gorchtein and C. J. Horowitz, Phys. Rev. Lett. **102** (2009) 091806.

[11] A. Sibirtsev, P. G. Blunden, W. Melnitchouk and A. W. Thomas, Phys. Rev. D **82** (2010) 013011.

[12] B. C. Rislow and C. E. Carlson, Phys. Rev. D **83** (2011) 113007.

[13] M. Gorchtein, C. J. Horowitz and M. J. Ramsey-Musolf, Phys. Rev. C **84** (2011) 015502.

[14] N. L. Hall, P. G. Blunden, W. Melnitchouk, A. W. Thomas and R. D. Young, Phys. Rev. D **88** (2013) 013011.

[15] D. Wang *et al.*, Phys. Rev. Lett. **111** (2013) 082501.

[16] D. Wang *et al.*, Nature **506** (2014) 67.

[17] W. Melnitchouk, R. Ent and C. E. Keppel, Phys. Rept. **406** (2005) 127.

[18] E. D. Bloom and F. J. Gilman, Phys. Rev. Lett. **25** (1970) 1140.

[19] E. D. Bloom and F. J. Gilman, Phys. Rev. D **4** (1971) 2901.

[20] I. Niculescu *et al.*, Phys. Rev. Lett. **85** (2000) 1186.

[21] I. Niculescu *et al.*, Phys. Rev. Lett. **85** (2000) 1182.

[22] A. Airapetian *et al.*, Phys. Rev. Lett. **90** (2003) 092002.

[23] J. Arrington, R. Ent, C. E. Keppel, J. Mammei and I. Niculescu, Phys. Rev. C **73** (2006) 035205.

[24] F. R. Wesselmann *et al.*, Phys. Rev. Lett. **98** (2007) 132003.

[25] A. Psaker, W. Melnitchouk, M. E. Christy and C. E. Keppel, Phys. Rev. C **78** (2008) 025206.

[26] S. P. Malace *et al.*, Phys. Rev. C **80** (2009) 035207.

[27] S. P. Malace, Y. Kahn, W. Melnitchouk and C. E. Keppel, Phys. Rev. Lett. **104** (2010) 102001.

[28] I. Niculescu *et al.*, Phys. Rev. C **91** (2015) 055206.

[29] J. Mammei, Nuovo Cim. C035N04 (2012) 203.

[30] F. Maas, talk presented at *PAVI 2014: From Parity Violation to Hadron Structure*, Skaneateles, New York, July 2014.

[31] A. De Rujula, H. Georgi and H. D. Politzer, Annals Phys. **103** (1977) 315.

[32] O. Nachtmann, Nucl. Phys. **B63** (1973) 237.

[33] O. Nachtmann, Nucl. Phys. **B78** (1974) 455.

[34] Note that the notation for $\mu_1^{(n)}$ and $\mu_2^{(n)}$ in Ref. [33] differs from that which we use in Eqs. (2) and (3).

[35] O. W. Greenberg and D. Bhaumik, Phys. Rev. D **4** (1971) 2048.

[36] J. M. Cornwall and R. E. Norton, Phys. Rev. **177** (1969) 2584.

[37] P. Monaghan *et al.*, Phys. Rev. Lett. **110** (2013) 152002.

[38] M. E. Christy and P. E. Bosted, Phys. Rev. C **81** (2010) 055213.

[39] S. Alekhin, J. Blümlein and S. Moch, Phys. Rev. D **86** (2012) 054009.

[40] F. M. Steffens and W. Melnitchouk, Phys. Rev. C **73** (2006) 055202.

[41] M. Virchaux and A. Milsztajn, Phys. Lett. B **274** (1992) 221.

[42] S. I. Alekhin, S. A. Kulagin and S. Liuti, Phys. Rev. D **69** (2004) 114009.

[43] P. Jimenez-Delgado and E. Reya, Phys. Rev. D **89** (2014) 074049.

[44] P. E. Bosted and M. E. Christy, Phys. Rev. C **77** (2008) 065206.

[45] J. F. Owens, A. Accardi and W. Melnitchouk, Phys. Rev. D **87** (2013) 094012.

[46] J. J. Kelly, Phys. Rev. C **70** (2004) 068202.

[47] X. D. Ji and P. Unrau, Phys. Rev. D **52** (1995) 72.

[48] F. D. Aaron *et al.*, JHEP **1209** (2012) 061; H. Abramowicz *et al.*, Phys. Rev. D **87** (2013) 052014.

[49] J. Alwall and G. Ingelman, Phys. Lett. B **596** (2004) 77.

[50] N. L. Hall, P. G. Blunden, W. Melnitchouk, A. W. Thomas and R. D. Young, Phys. Lett. B **731** (2014) 287.

[51] J. J. Sakurai and D. Schildknecht, Phys. Lett. B **40** (1972) 121.